THE JOURNAL OF BIOLOGICAL CHEMISTRY VOL. 284, NO. 42, pp. 28599–28606, October 16, 2009

Regulation of Immature Dendritic Cell Migration by RhoA Guanine Nucleotide Exchange Factor Arhgef5*[S]

Received for publication, July 21, 2009, and in revised form, August 26, 2009 Published, JBC Papers in Press, August 27, 2009, DOI 10.1074/jbc.M109.047282

Zhenglong Wang[‡], Yosuke Kumamoto[§], Ping Wang[‡], Xiaoqing Gan[‡], David Lehmann[¶], Alan V. Smrcka[¶], Lauren Cohn[‖], Akiko Iwasaki[§], Lin Li[1], and Dianqing Wu[‡2]**

*From the [‡]Program for Vascular Biology and Therapeutics and Department of Pharmacology, the [§]Department of Immunobiology, and the [‖]Section of Pulmonary and Critical Care Medicine, Yale University School of Medicine, New Haven, Connecticut 06520, the [¶]Department of Pharmacology, University of Rochester, Rochester, New York 14642, and the **State Key Laboratory of Molecular Biology, Institute of Biochemistry and Cell Biology, Shanghai Institutes for Biological Sciences, Chinese Academy of Sciences, Shanghai 200031, China*

There are a large number of Rho guanine nucleotide exchange factors, most of which have no known functions. Here, we carried out a short hairpin RNA-based functional screen of RhoGEFs for their roles in leukocyte chemotaxis and identified Arhgef5 as an important factor in chemotaxis of a macrophage phage-like RAW264.7 cell line. Arhgef5 can strongly activate RhoA and RhoB and weakly RhoC and RhoG, but not Rac1, RhoQ, RhoD, or RhoV, in transfected human embryonic kidney 293 cells. In addition, Gβγ interacts with Arhgef5 and can stimulate Arhgef5-mediated activation of RhoA in an *in vitro* assay. *In vivo* roles of Arhgef5 were investigated using an Arhgef-5-null mouse line. Arhgef5 deficiency did not affect chemotaxis of mouse macrophages, T and B lymphocytes, and bone marrow-derived mature dendritic cells (DC), but it abrogated MIP1α-induced chemotaxis of immature DCs and impaired migration of DCs from the skin to lymph node. In addition, Arhgef5 deficiency attenuated allergic airway inflammation. Therefore, this study provides new insights into signaling mechanisms for DC migration regulation.

Leukocyte chemotaxis underlies leukocyte migration, infiltration, trafficking, and homing that are not only important for normal leukocyte functions, but also have a important role in inflammation-related diseases. Leukocyte chemotaxis is regulated by leukocyte chemoattractants that include bacterial byproducts such as formylmethionylleucylphenylalanine, complement proteolytic fragments such as C5a, and the superfamily of chemotactic cytokines, chemokines. These chemoattractants bind to their specific cell G protein-coupled receptors and are primarily coupled to the G_i family of G proteins to regulate leukocyte chemotaxis. Previous studies have established that the Rho family of small GTPases regulates leukocyte migration (1, 2). Rac, Cdc42, and RhoA are the three best studied Rho small GTPases. In myeloid cells, Cdc42 regulates directionality by directing where F-actin and lamellipodia are formed, and Rac regulates F-actin formation in the lamellipodia, which provides a driving force for cell motility (3–6). On the other hand, RhoA regulates the formation and contractility of the actomyosin structure at the back that provides a pushing force (5, 7). Rho guanine nucleotide exchange factors (GEF)[3] are key regulators for the activity of these small GTPases. GEFs activate small GTPases by promoting the loading of GTP to the small GTPases, a rate-limiting step in GTPase regulation (8–11). Previous biochemical and genetic studies have revealed how Cdc42 and Rac may be regulated by chemokine receptors in leukocytes. Chemokine receptors can regulate Cdc42 via a Rho-GEF PIXα, which is regulated by Gβγ from the G_i proteins via the interactions between Gβγ and Pak1 and between Pak1 and PIXα in myeloid cells 12. On the other hand, in neutrophils chemokine receptors regulate Rac2 via another Rho-GEF P-Rex1, which is directly regulated by Gβγ (13–15). Two Rho-GEFs have been implicated in regulation of RhoA in neutrophils. GEF115 was found in the leading edges of polarized mouse neutrophils, whereas PDZ Rho-GEF was found in the uropods of differentiated HL-60 cells. Both Rho-GEFs were believed to mediate pertussis toxin-resistant activation of RhoA in these cells. However, a significant portion of RhoA activity in leukocytes are pertussis toxin-sensitive, which is presumably regulated by the α and/or βγ subunits from the G_i proteins. The signaling mechanism for this pertussis toxin-sensitive RhoA regulation by chemokine receptors remains largely elusive.

Molecular cloning and genomic sequencing have identified more than 70 Rho-GEFs in mammals (16–20). Many of these Rho-GEFs have been shown to activate RhoA in *in vitro* and overexpression assays (16–20). However, it is not known if any of them regulate RhoA *in vivo*, we have found that PIXα is a specific GEF for Cdcd42 in neutrophils (12) despite its potent activity on Rac in *in vitro* and overexpression assays (21, 22).

* This work was supported, in whole or in part, by National Institutes of Health Grants HL080706 and HL070694 (to D. W.), grants from the American Heart Association (to P. W.), Ministry of Science and Technology of China Grant 2002CB513000, and National Science Foundation of China Grant 30521005 (to L. L.).

[S] The on-line version of this article (available at http://www.jbc.org) contains supplemental Table S1 and Fig. S1.

[1] To whom correspondence may be addressed. E-mail: lli@sibs.ac.cn.

[2] To whom correspondence may be addressed. E-mail: Dan.Wu@Yale.edu.

[3] The abbreviations used are: GEF, guanine nucleotide exchange factors; siRNA, small interfering RNA; shRNA, short hairpin RNA; DC, dendritic cell; RBD, Rho-binding domain; PAK, p21-binding domain; GST, glutathione *S*-transferase; BAL, bronchoalveolar lavage; HSV, herpes simplex virus type 2; MFI, mean fluorescence intensity; PH, pleckstrin homology; HA, hemagglutinin; GFP, green fluorescent protein; ELISA, enzyme-linked immunosorbent assay; IL, interleukin; FITC, fluorescein isothiocyanate; HEK, human embryonic kidney; RT, reverse transcriptase; OVA, ovalbumin; IFN, interferon; Mant, *N*-methylanthraniloyl; DH, Dbl homology; MIP-1α, macrophage inflammatory protein-1α; SDF-1, stromal-derived factor-1.

Therefore, we used a siRNA-based loss of function screen in an attempt to identify the GEFs that regulate myeloid cell migration and RhoA activity. One of the candidates, Arhgef5, was found to be directly activated by $G\beta\gamma$ to regulate RhoA and has an important role in immature DC migration. In addition, Arhgef5 deficiency attenuated allergic airway inflammation in a mouse model.

MATERIALS AND METHODS

Plasmids, Protein Preparation, Cell Culture, and Transfection—The full-length Arhgef5 cDNA and its truncated mutants were amplified and subcloned into a mammalian expression vector carrying a FLAG tag. The exchange activity-deficient Arhgef5 mutant Arhgef5DH was generated by substituting Ala residues for Leu^{245} and Leu^{246}. For the *in vitro* binding assay, Arhgef5 cDNA was subcloned into the pET21-His vector. His-tagged Arhgef5 was expressed in BL21(DE3)-competent cells and subsequently purified with nickel-nitrilotriacetic acid (Qiagen). Recombinant RhoA, Rhoteckin-RBD, and PAK-PBD, and Elmo were prepared from bacteria as GST fusion proteins. The $G\beta1\gamma2$ protein was prepared as previously described (12). The cDNAs of RhoB, RhoC, RhoD, RhoG, and RhoQ as well as the dominant negative forms of RhoC, RhoD, and RhoF were acquired from the Missouri S&T cDNA Resources Center carrying an HA tag at their N termini. DNA sequences of all expression constructs were verified by sequencing. Antibodies specific to HA, His, and FLAG were acquired from Covance.

HEK293T cells and Raw264.7 cells were maintained in Dulbecco's modified Eagle's medium (Cellgro) supplemented with penicillin/streptomycin and 10% fetal bovine serum (Hyclone). The B lymphoid cells were cultured in RPMI 1640 medium (Cellgro) supplemented with penicillin/streptomycin and 10% heat-inactivated fetal bovine serum (Hyclone). Transfection was carried out using Lipofectamine Plus (Invitrogen) following the manufacturer's instructions.

The method to culture immature and mature dendritic cells from mouse bone marrow was described in detail (44). Briefly, mouse bone marrow cells were collected by flushing the femurs. After lysis of the red blood cells, the cells were cultured in the Dulbecco's modified Eagle's medium supplemented with 20 ng/ml mouse recombinant granulocyte macrophage colony-stimulating factor (PeproTech). After 5 days, cultured cells were collected and used for immature DC migration assays. Alternatively, the immature DCs were treated with 1 μg/ml lipopolysaccharide (Sigma) for 24 h and used for mature DC migration assays.

shRNAs Screening and Chemotaxis Assays—The shRNA vector, which was named pAS, was modified based on pSuper (23) by incorporating a GFP-luciferase fusion protein expression unit. The sequences for these shRNAs are shown in supplemental Table S1. For screening, the shRNAs and control vector were transfected into Raw264.7 cells using Lipofectamine Plus. The cells were collected 48 h later by trypsinization and resuspended in Dulbecco's modified Eagle's medium containing 1% fetal bovine serum. They were then loaded into the upper chambers of 24-well transwell plates (Costar, 5 μM pore size). The lower chambers were filled with the same medium, but supplemented with 10 nM C5a (Sigma). The plates were incubated at 37 °C for 4 h. Migrated cells were detached from the lower surface of the transwell inserts by trypsin and EDTA and lysed for luciferase assays. The chemotactic indices were calculated by dividing the luciferase activity of migrated cells in the presence of C5a by that of its absence.

For DC migration assays, BM-derived immature DCs or mature DCs were collected and resuspended in Dulbecco's modified Eagle's medium containing 1% fetal bovine serum and loaded onto the upper chambers of transwell plates. Immature DCs were stimulated with 300 ng/ml MIP-1α (PeproTech), whereas mature DCs were stimulated with 60 ng/ml CCL-19 (PeproTech) for 4 h at 37 °C. Migrated cells were then counted and stained with CD11c for flow cytometric analysis. The chemotaxis indices were calculated by dividing the number of migrated immature ($CD11c^{mid}$) or mature ($CD11c^{high}$) DCs in the presence of a chemotactic ligand by that in its absence.

To evaluate the role of Arhgef5 and -15 in mature DC chemotaxis, bone marrow-derived immature DCs were collected and transfected with synthetic siRNA duplex oligos of Arhgef5 and Arhgef15 using the Amaxa Nucleofector system (Amaxa Inc.). Twenty-four hours after transfection, lipopolysaccharide was added into the culture to induce DC maturation. Mature DCs were collected for the transwell migration assay as described above 24 h after the induction. The target sequences for the Arhgef5 and Arhgef15 siRNAs were CAGGAGGAATTTAATAATACA and AAGTATTAAATTAATCTAATA, respectively.

For evaluating lymphocyte migration, splenocytes were used in the transwell assay in response to 10 nM SDF-1. After 3 h incubation at 37 °C, migrated cells were counted and stained with anti-CD3-FITC and anti-B220-R-phycoerythrin. The numbers of migrated T and B cells were determined based on the cell number and their relative percentages, and chemotactic indices were computed as described above. For macrophage chemotaxis assay, macrophages were obtained from the mouse peritonea elicited by thioglycolate. Similar transwell assays were carried out with 10 nM C5a (Sigma) as the stimulus.

GTPase Pulldown Assays—The pulldown assays for determining the activity of small GTPases were carried essentially as previously described. In brief, HEK293T cells were cotransfected with Arhgef5 or its inactive mutant Arhgef5DH with one of the HA-tagged small GTPases. After 24 h transfection, cells were lysed with the lysis buffer (50 mM Tris-HCl (pH 7.3), 10 mM $MgCl_2$ and 0.2 M NaCl, 2% Nonidet P-40, 10% glycerol, 2 mM orthovanadate) containing recombinant GST-Rhoteckin-RBD for RhoA, RhoB, and RhoC pulldown, GST-PAK-CRIB for Rac, RhoD, and RhoQ pulldown, or GST-Elmo for RhoG pulldown. Bound GTPases were detected by Western analysis with an anti-HA antibody.

RBD Binding Assay—Cells were stimulated with or without 30 ng/ml SDF-1 for 15 s before they were fixed with 4% paraformaldehyde. The cells were then washed and permeabilized by 0.1% Triton X-100 at room temperature for 5 min. After washing, cells were blocked by 1% bovine serum albumin and incubated with purified GST-RBD at room temperature for 1 h followed by Alexa 633-conjugated anti-GST antibody (Molecular Probes, Inc.). After washing, cells were analyzed by

a flow cytometer, and the mean fluorescence intensity (MFI) of GFP-positive populations that represent cells carrying the pAS vector was determined.

Guanine Nucleotide Loading Assays—The exchange activity of Arhgef5 was determine for its ability to promote the loading of *N*-methylanthraniloyl-GTP (Mant-GTP, from JENA Bioscience) to recombinant RhoA as previously described (45). In brief, purified RhoA (0.12 μM) was incubated in an assay buffer containing 20 mM Tris (pH 7.5), 150 mM NaCl, 5 mM $MgCl_2$, and 1 mM dithiothreitol with 10 μM MANT-GTP and recombinant proteins of 0.85 μM Arhgef5 and/or 1 μM G$\beta\gamma$. Immediately after mixing, fluorescence intensity was determined by a fluorometer (Wallac Vector, 1420 multilabel counter) with excitation wavelength of 360 nm and emission wavelength of 440 nm.

Luciferase Reporter Assays—HEK293T cells were seeded in 24-well culture plates and transfected with the luciferase reporter construct SRE-luc, normalization plasmid GFP, and other plasmids shown in the figures by using Lipofectamine Plus. After transfection, cells were cultured in serum-free medium for 24 h before the GFP intensity was measured by a fluorometer. The cells were then lysed, and their luciferase activities were determined by a luminometer. Data are presented after the luciferase activity was normalized against the GFP intensity.

Immunoprecipitation—HEK293T cells were cotransfected with Gβ1γ2 and FLAG-tagged Arhgef5 or its mutants for 24 h. The cells were lysed with a lysis buffer (1% Nonidet P-40, 1% sodium deoxycholate, 0.1% SDS, 0.15 M NaCl, 0.01 M sodium phosphate, 50 mM sodium fluoride, 2 mM EDTA, pH 7.2). Immunoprecipitation was then carried out with an anti-FLAG antibody and Protein A/G beads at 4 °C for 1 h. The immunocomplexes were subjected to Western analysis with anti-Gβ1 antibody.

RT-PCR—Total RNAs were extracted from bone marrow-derived immature and mature DCs using the TRIzol reagent (Invitrogen) according to the manufacturer's instructions. RNA was reverse-transcribed using the iScript cDNA synthesis kit (Bio-Rad). RT-PCR was performed. The sense oligo for Ephexin is GAACTGATCGCACAGTTGGA, and the antisense oligo is ATCTTCCGGACACCCTCATT. The sense oligo for Arhgef15 is ATCACTCAGCCCA-AGAGTGG, and the antisense oligo is AGATGGTGTCTGGGGAACAG. The sense oligo for Arhgef5 is TATGTCACCAACCAGACC, and the antisense oligo is ACCTGACTGATGAAGTTCCT.

In Vivo DC Migration Assay—The migration of DCs from the skin to lymph node was determined by FITC skin painting as previously described (46). In brief, FITC (Sigma) was dissolved in a 50:50 (v/v) acetone/dibutylphthalate mixture at a concentration of 5 mg/ml. Mice were anesthetized and their abdominal fur shaved. The FITC solution (0.25 ml/animal) was applied to the shaved skin. Twenty-four hours later, inguinal lymph nodes were harvested and treated with collagenase D (1 mg/ml, Roche) for 20 min at 37 °C. The lymph nodes were then smashed onto 70 μM cell strainers to produce cell suspensions. The cells were collected and stained with PE-CD11c and analyzed by a flow cytometer.

Generation of Arhgef5-null Mice—A BAC clone that contains the *Arhgef5* gene was acquired from the BACPAC Resources Center at the Children's Hospital Oakland Research Institute, Oakland, CA. Exons 5–9, which encode residues Ala^{1153}–Lys^{1355} in the DH domain of Arhgef5, were floxed with the LoxP sequences in the gene-targeting construct. The Arhgef5 mutant mouse line was generated at the Gene Targeting and Transgenic Facility of the University of Connecticut Health Center using the ES cell line 129S6 derived from 129SvEvTac/C57BL/6J F1 blastocysts. The chimeric mice were crossed with 129S1-Hprt1-Cre from JAX to produce germline excision of the sequences between the two LoxP sites. Finally, mice heterozygous for the disrupted *Arhgef5* gene were interbred to produce homozygous mice. Animals from F1 to F3 were used in this study.

Ovalbumin-induced Asthma Model—Mice were sensitized by intraperitoneal injection with 200 μl of OVA-alum suspension (0.5 mg/ml ovalbumin (OVA, Sigma) in phosphate-buffered saline mixed with an equal volume of 20 mg/ml aluminum hydroxide). Eight days after immunization, mice were challenged with an aerosol of 1% FITC-OVA in phosphate-buffered saline, delivered by an ultrasonic nebulizer (OMRON, Compair) for 20 min. FITC-OVA was prepared by mixing 2 mg/ml of FITC solution in carbonate buffer (220 mM, pH 9.6) with OVA at 10 mg/ml. The mixture was gently rotated overnight at 4 °C in the dark. Unbound FITC was removed by ultrafiltration using a 10-kDa molecular mass cut-off membrane in a 15-ml filtration cell (Amicon). One day after challenge, the mice were anesthetized. Their trachea were cannulated, and their lungs lavaged five times with 1 ml of pre-chilled phosphate-buffered saline. The bronchial lymph nodes were then collected. Cells in the bronchoalveolar lavage (BAL) fluid were collected by centrifugation at 4000 $\times$ *g* for 5 min. Cytospin preparations of cells were stained with Diff-Quik (Dade Behring) and differentials were performed on 200 cells based on morphology and staining characteristics. The supernatant of BAL fluids were analyzed for IL-4 levels using a mouse IL-4 ELISA kit (Endogen). Lymph nodes were passed through a cell strainer (BD Falcon), and cells were counted and stained with R-phycoerythrin-CD11c (BD Pharmingen) and analyzed by a flow cytometry (Caliber, BD Biosciences).

Intravaginal Infection of Herpes Simplex Virus Type 2 (HSV-2)—The thymidine kinase mutant HSV-2 viruses were prepared and inoculated intravaginally into Arhgef5-null and wild type littermates (1×10^6 plaque-forming units of HSV-2) as previously described (47). Vaginal washes were collected daily, and the levels of IFN-γ and IL-12 were determined by ELISA. On day 6, mice were euthanized, and $CD4^+$ or $CD8^+$ T cells were isolated from iliac and inguinal lymph nodes. The T cells were co-cultured with naïve wild type splenocytes and heat-inactivated HSV-2 of varying plaque-forming units (for $CD4^+$ T cells) or 1 μg/ml gB peptide (for $CD8^+$ T cells) for 3 days. The levels of IFN-γ in the conditioned media were determined by ELISA.

Statistical Analysis—Statistical comparisons between different groups or treatments were performed by unpaired two-tailed Student's *t* test and $p < 0.05$ was considered statistically significant.

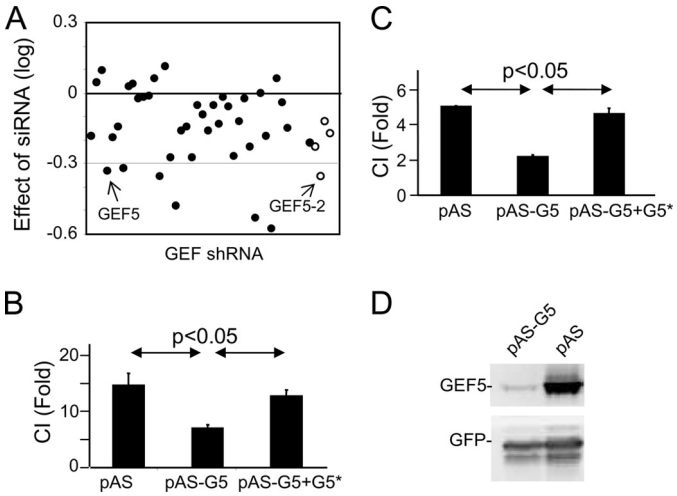

FIGURE 1. **Effects of GEF shRNAs on chemotaxis.** *A*, effects of the GEF shRNAs on RAW264.7 cell chemotaxis in response to C5a. The chemotactic index of cells expressing pAS is taken as 1, and the relative chemotactic activity of cells expressing each GEF shRNA was calculated. Data shown are log of the relative chemotactic activities. The raw data are shown in supplemental Table S1. The *open circles* denote the second shRNAs used for validation of the initial hits. *B* and *C*, rescuing the effect of Arhgef5 shRNA by expressing an Arhgef5 mutant containing a silent mutation. Raw 264.7 cells (*B*) and J774 cells (*C*) were cotransfected with pAS, Arhgef5 shRNA (*pAS-G5*), and/or silently mutated Arhgef5 (*G5**) for 48 h. Chemotactic assays were carried out using the transwell plate in the presence of C5a for RAW264.7 cells and SDF-1 for J774 cells. *CI* stands for chemotactic index. *D*, Arhgef5 shRNA validation. HEK293T cells were cotransfected with the plasmids expressing Arhgef5 and GFP and pAS or pAS-G5. Western analyses were carried out 2 days after transfection.

RESULTS

To investigate the roles of Rho-GEFs in leukocyte chemotaxis, we carried out a siRNA-based functional screen for Rho-GEFs that may play a role in migration of macrophage-like Raw264.7 cells. We generated a mini vector-based shRNA library targeting 38 Rho-GEFs, whose expression could be detected by RT-PCR in RAW264.7 cells (data not shown). The shRNA vector was modified based on pSuper (23) by incorporating a GFP-luciferase fusion protein expression unit; thus, cells producing shRNA can be monitored by the expression of GFP and/or luciferase. This vector was named pAS. All of the GEF shRNAs were validated based their ability to knock down endogenous GEF expression detected by quantitative RT-PCR and/or coexpressed cDNAs if available (data not shown). To test the effects of these shRNAs on RAW264.7 cell migration, cells were transfected with one of the shRNAs, and the empty pAS was used as a negative control. Two days after transfection, transwell migration assays were carried out, and the migratory ability of the cells expressing a GEF shRNA was compared with that of the control cells. Of 38 GEF shRNAs we screened, 6 shRNAs showed more than 50% inhibition (Fig. 1*A* and supplemental Table S1). Because siRNAs are known to have off-target effects, we tried to validate the effects by constructing a second shRNA expression plasmid that has a different targeting sequence for these 6 putative hits. We successfully generated the second shRNAs for 5 of these 6 putative hits. Among these 5 shRNAs, only Arhgef5 shRNA showed more than 50% inhibition of RAW264.7 cell migration (supplemental Table S1 and Fig. 1*A*). To further validate siRNA specificity, we coexpressed an Arhgef5 expression plasmid together with its shRNA plasmid to determine whether effects of shRNA can be rescued. To prevent the silencing effect of the shRNA on expression of exogenous Arhgef5, we introduced silent mutations at the shRNA targeting sequence of the Arhgef5 cDNA. As shown in Fig. 1*B*, expression of Arhgef5 effectively rescued the effect of Arhgef5 shRNA on RAW264.7 cell migration. We also tested the effect of Arhgef5 shRNA on the migration of J774 cells; the shRNA could also effectively inhibit its migration, which could be rescued by expression of the silently mutated Arhgef5 (Fig. 1*C*). The efficiency of this Arhgef5 siRNA was validated as shown in Fig. 1*D*. Putting all of these results together, we believe that Arhgef5 may have an important role in the migration of these two myeloid cell lines.

Arhgef5, as a member of the Rho-GEF superfamily, possesses a DH-PH tandem domain and a C-terminal SH3 domain. Some members of the subfamily, including Arhgef15 (24), Ephexin-1 (25), and Arhgef5 (26), were shown to activate RhoA, whereas the other (SGEF) was shown to activate RhoG (27). We tested the effects of Arhgef5 on a number of Rho small GTPases. Previous studies have shown that the RhoA-binding domain of Rhotekin (RBD) has a high affinity for a subset of GTP-bound small Rho GTPases that include RhoA, RhoB, and RhoC (28, 29), whereas the p21-binding domain of PAK1 (PBD) has a high affinity for Rac, RhoQ, RhoD, and RhoV (29, 30). Active RhoG was found to be bound to Elmo (31). These interactions have been used to determine the levels of active small GTPases in pulldown assays (28–30). As shown in Fig. 2*A*, expression of Arhgef5, but not an Arhgef5 mutant with its DH domain mutated, led to a strong increase in the levels of active RhoA and RhoB, resulting in weak activation of RhoC and RhoG. Expression of Arhgef5 had no effect on the level of active RhoD, RhoV, RhoQ, or Rac1 (Fig. 2*A*). Previous studies also showed that GEFs generally exhibit high affinities for the GTP-free mutant forms of small GTPases they regulate (32, 33). Consistent with the pulldown assay results, Arhgef5 co-immunoprecipitated with RhoA-N^{19}, but not RhoC-N^{19} or RhoD-N^{31} (Fig. 2*B*). In addition, RhoF-N^{33} did not show detectable interaction with Arhgef5 (Fig. 2*B*), suggesting that Arhgef5 may not regulate RhoF. These results indicate that Arhgef5, Ephexin-1, and Arhgef15, which are more homologous in amino acid sequences than SGEF, belong to a subgroup that potently activates RhoA rather than RhoG.

Next, we wanted to assess the significance of Arhgef5 in chemoattractant-induced small GTPase activation. Because of the relative low transfection efficiency for leukocytes and the large number of cells required for the pulldown assays particularly for detection of endogenous proteins, we developed a flow cytometry-based approach to assess the GTPase activities. J774 cells expressing Arhgef5 shRNA (G5pAS) or the control vector (pAS) were stimulated with SDF-1. They were then fixed, permeabilized, and incubated with purified GST-RBD and Alexa 633-conjugated anti-GST antibody. The MFI of GFP-positive populations that represent cells carrying the pAS vector was determined by a flow cytometer. As shown in Fig. 2*C*, SDF-1 treatment resulted in a marked right-shift in MFI in cells expressing the control vector, suggesting that SDF-1 stimulates the activation of small GTPase that can bind to RBD in these

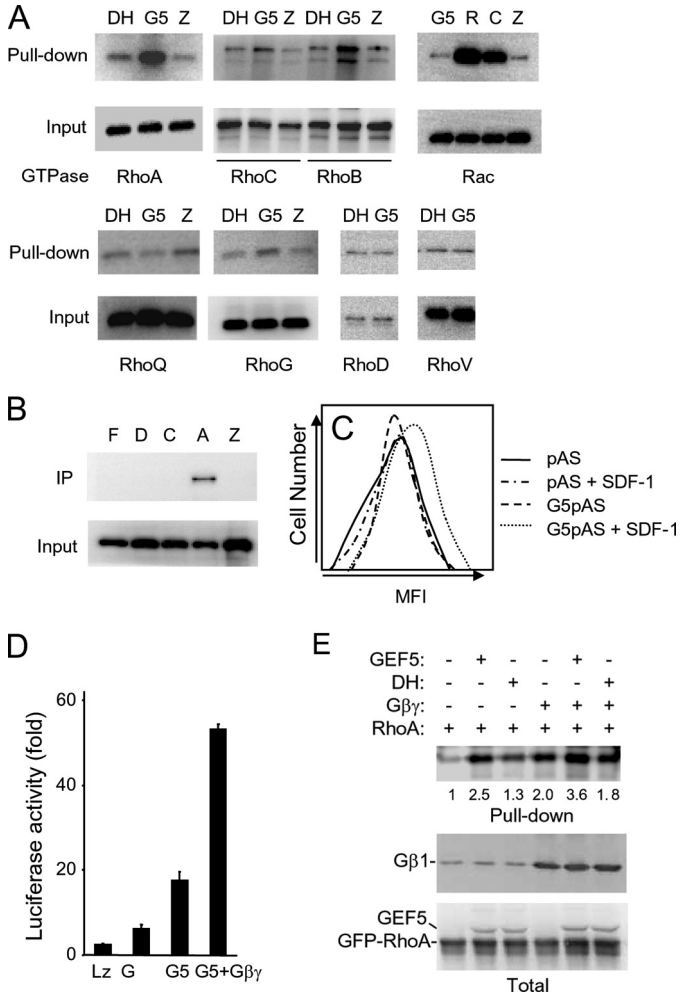

FIGURE 2. **Regulation of Rho small GTPases by Arhgef5.** *A*, pulldown assays. HEK293T cells were cotransfected with one of the small GTPases and LacZ (*Z*), Arhgef5 (*G5*), or the loss-of-function mutant of Arhgef5 (*DH*). The RBD pulldown assays were carried out for cells expressing RhoA, RhoB, and RhoC, whereas the PBD pulldown assay was done for Rac, RhoQ, RhoD, and RhoV. The activity of RhoG was determined by a pulldown using GST-Elmo. Both precipitated and total GTPases were detected by Western analysis using an antibody specific for the HA tag carried by these small GTPases. *B*, interaction of dominant negative GTPases with Arhgef5. HA-tagged RhoA-N^{19} (*A*), RhoC-N^{19} (*C*), RhoD-N^{31} (*D*), RhoF-N^{33} (*F*), and LacZ were cotransfected with FLAG-tagged Arhgef5 in HEK293T cells. Immunoprecipitation (*IP*) was carried out with an anti-HA antibody and detected with an anti-FLAG antibody. *C*, knocking down Arhgef5 reduced SDF-1-induced RBD binding. J774 cells were transfected with pAS or Arhgef5 shRNA for 48 h and stimulated with or without 30 ng/ml SDF-1 for 15 s. Cells were fixed, permeabilized, stained with GST-RBD and Alexa 633-labeled secondary antibody, and analyzed by a flow cytometer. MFI of Alexa 633 in cells gated for GFP is shown. Three experiments were performed. A representative one is shown. *D*, SRE.L-luciferase assay. HEK293T cells were co-transfected with the SRE-luciferase reporter gene, GFP, LacZ, G$\beta\gamma$, and/or Arhgef5. Cells were lysed and the GFP levels and luciferase activity were determined. The luciferase activity was normalized against the GFP level. *E*, activation of RhoA by G$\beta\gamma$ and Ahrgef5 in a cotransfection assay. HEF293T cells were transfected as indicated. Twenty-four hours later, RBD pulldown assays were carried out. The *numbers under* the *top panel* are relative band intensity quantified by densitometry and normalized against total RhoA levels.

cells. However, in cells expressing Arhgef5 shRNA, the SDF-1-induced MFI increase was blunted (Fig. 2*C*). This result suggests that Arhgef5 has a significant role in regulation of endogenous Rho GTPases.

Because RhoA and its close homolog RhoB can be potently activated by Arhgef5, we interpret the inhibitory effect of the Arhgef5 shRNA on RBD binding to suggest that Arhgef5 may be involved in chemoattractant-mediated activation of RhoA and/or RhoB. In leukocytes, G$\beta\gamma$ subunits have been shown to mediate many of the chemoattractant signaling events. Thus, we examined if G$\beta\gamma$ regulates Arhgef5. We first performed the SRE.L-luciferase reporter gene assay, which was previously shown to be specifically activated by Rho GTPases (15, 34–36). As shown in Fig. 2*D*, coexpression of G$\beta1\gamma2$ and Arhgef5 led to synergistic activation of the reporter gene activity, suggesting that G$\beta\gamma$ and Arhgef5 may function in the same signaling pathway. This conclusion is supported by the observation that coexpression of Arhgef5, G$\beta1\gamma2$, and RhoA led to the highest levels of active RhoA (Fig. 2*E*).

To further investigate the relationship between G$\beta\gamma$ and Arhgef5, we examined if G$\beta\gamma$ can interact with Arhgef5 in an immunoprecipitation assay. We found that G$\beta\gamma$ and Arhgef5 coimmunoprecipitated in HEK293 cells expressing both proteins (Fig. 3, *A* and *B*). We went on to delineate the sequences on Arhgef5 that are required for its interaction with G$\beta\gamma$. A series of Arhgef5 deletion mutants were generated as depicted in Fig. 3*A*. These Arhgef5 mutants were tested for their ability to coimmunoprecipitate with G$\beta1\gamma2$ in HEK293 cells. We found that the sequence encompassing residues Val^{281}–Thr^{395} is minimal for retaining the full ability to interact with G$\beta\gamma$ (Fig. 3*B*). The fact that the sequences encompassing residues Val^{281}–Arg^{311} and Trp^{312}–Glu^{424} are also able to bind to G$\beta\gamma$ (Fig. 3*B*) support the idea that the G$\beta\gamma$-binding site is located in and near the PH domain. To determine whether the interaction between G$\beta\gamma$ and Arhgef5 is direct, we carried out an *in vitro* pulldown assay using recombinant Arhgef5 protein prepared from a bacterial expression system and G$\beta1\gamma2$ protein prepared from a baculoviral expression system. The pulldown assay shows that these two proteins can interact directly (Fig. 3*C*).

The aforementioned results together suggest that G$\beta\gamma$ binds to and may activate Arhgef5, which in turn activates RhoA. To demonstrate that G$\beta\gamma$ can activate RhoA via Arhgef5 in a biochemically defined system, we carried out an *in vitro* GTP loading assay. In this assay, we tested if recombinant G$\beta1\gamma2$ and Arhgef5 proteins were able to stimulate the loading of a fluorogenic GTP analog, Mant-GTP (37), to recombinant RhoA, which represents the activation of the small GTPase. We found that, whereas Arhgef5 alone stimulated GTP loading to RhoA as expected, addition of G$\beta1\gamma2$ resulted in a further increase in GTP loading (Fig. 3*D*) and that G$\beta1\gamma2$ regulated this RhoA activity in a dose-dependent manner (Fig. 3*E*). These results demonstrate that G$\beta\gamma$ is able to directly activate Arhgef5, which in turn activates RhoA.

Next we investigated the roles that Arhgef5 plays *in vivo* by generating a mouse line in which the *Arhgef5* gene was disrupted (supplemental Fig. S1). Because siRNA-mediated knocking down of Arhgef5 expression led to impaired chemotaxis of a macrophage, we first examined whether Arhgef5 deficiency affected the primary mouse macrophage chemotaxis. The migration of neither peritoneal macrophages in response to C5a was, however, not affected (Fig. 4*A*). We also examined chemotaxis of spleen T and B lymphocytes in response to SDF-1 and bone marrow neutrophils

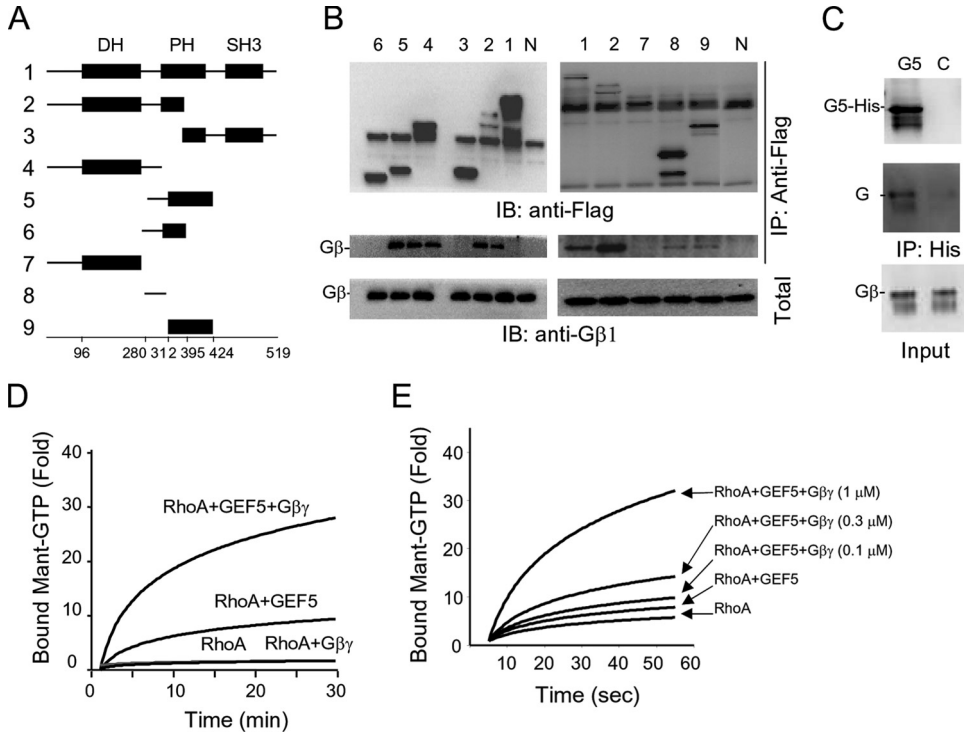

FIGURE 3. **Gβγ interacts with and directly activates Arhgef5.** *A*, schematic representation of Arhgef5 and its mutants. The diagrams are not drawn in scale. The *numbers at the side* correspond to those in *B*. *B*, interaction of Gβγ with Arhgef5 and its deletion mutants. FLAG-tagged Arhgef5 and its mutant were cotransfected with Gβ1γ2 in HEK293T cells. Immunoprecipitation (*IP*) was carried out using the anti-FLAG antibody and detected using an anti-Gβ1 antibody. *N*, no Arhgef5 transfected. *C*, direct interaction between Arhgef5 and Gβ1γ2. His-tagged Arhgef5 protein purified from a bacterial expression system was incubated with Gβγ from a baculoviral expression system. Pulldown was carried out by an anti-His antibody and detected by an anti-Gβ1 antibody. *D*, direct regulation of Arhgef5 by Gβ1γ2. Purified recombinant proteins of Gβ1γ2 (1 μM), Arhgef5 (0.5 μM), and/or RhoA (0.12 μM) were incubated as indicated in the figure in the presence of Mant-GTP. *E*, dose-dependent activation of RhoA by Gβγ. Different doses of Gβ1γ2 were incubated with RhoA (0.12 μM) and Arhgef5 (0.5 μM). *IB*, immunoblot.

We postulated that the lack of effect of Arhgef5 deficiency on mature DC migration may be due to the molecular redundancy as there are several Arhgef5 close homologues whose expression may be up-regulated in mature DCs to functionally compensate the lack of Arhgef5. Therefore, we examined the expression of Arhgef5 and its two homologs Ephexin-1 and Arhgef15 in immature and mature DCs. Although Arhgef5 could be detected in both mature and immature DCs, Ephexin-1 and Arhgef15 could only be detected in mature DCs by RT-PCR (Fig. 4*G*), suggesting that the relative contribution of Arhgef5 may diminish along with the increases in Ephexin-1 and Arhgef15 expression during DC maturation. To test whether these Arhgef5 homologs are indeed a functional redundancy in regulation of mature DC migration, we attempted knocking down of Arhgef5, Arhgef15, and both in cultured mature DCs with their specific siRNAs. As shown in Fig. 4*H*, transfection of mouse bone marrow-derived mature DCs with both siRNAs led a significant reduction in mature DC chemotaxis in response to CCL-19, although the transfection of either siRNA alone showed insignificant effects.

to formylmethionylleucylphenylalanine. Arhgef5 deficiency did not affect the chemotactic responses of these cells (Fig. 4*B*, data not shown).

DCs play important roles in modulating in the adapted immune system, and some of them share the same ontogeny as macrophages (38, 39). Therefore, we examined chemotaxis of bone marrow-derived immature DCs *in vitro* and found that Arhgef5 deficiency markedly impaired immature DC chemotaxis in response to MIP-1α (Fig. 4*C*). We also examined RhoA activation in response to MIP-1α and found that MIP-1α-induced RhoA activation is significantly reduced in the immature DCs from Arhgef5-null mice compared with those from wild type littermates (Fig. 4*D*). These results indicate that chemokines may regulate immature DC migration via Arhgef5 and RhoA. However, when we examined the effect of Arhgef5 deficiency on migration of mature DCs, we found that the lack of Arhgef5 had little effect (Fig. 4*D*). We also examined DC migration *in vivo* using the skin painting assay. There was a partial (35%), but statistically significant reduction in DC migration from the skin to lymph nodes in Arhgef5-null mice compared with the wild type controls (Fig. 4*F*). Because DCs start to mature upon antigen engagement, the differential effects of Arhgef5 deficiency on immature and mature DCs may explain this less robust effect of Arhgef5 deficiency on DC migration *in vivo*.

We also investigated the *in vivo* roles of Arhgef5 using two mouse model systems in which DCs are known to be involved: ovalbumin-induced allergic airway inflammation and vaginal infection of HSV-2. After OVA immunization and OVA challenge, we found that Arhgef5 deficiency reduced the number of eosinophils infiltrating into the respiratory tract, $CD11c^+$ DC cells migrating to the bronchial lymph node, and the levels of IL-4 in the BAL (Fig. 5, *A–C*). However, Arhgef5 deficiency did not cause significant changes in the levels of IL-12 or IFN-γ in vaginal washes. Furthermore, induction and differentiation of CD4 T cells as measured by IFN-γ production from $CD4^+$ T cells stimulated by heat-inactivated HSV-2 or CD8+ T cells by the gB peptide in the HSV-2 infection model were not significantly affected in Arhgef5-deficient mice (Fig. 5, *D–F*). These results suggest that Arhgef5 deficiency may affect the T_h2 responses in an OVA-induced asthma model, but not T_h1 responses induced following viral infection with HSV-2. In addition, the results shown in Fig. 5*F* indicate that intrinsic T cell responses are not affected by Arhgef5 deficiency.

DISCUSSION

We screened a mini-Rho-GEF shRNA library and identified Arhgef5 as an important GEF in the regulation of cul-

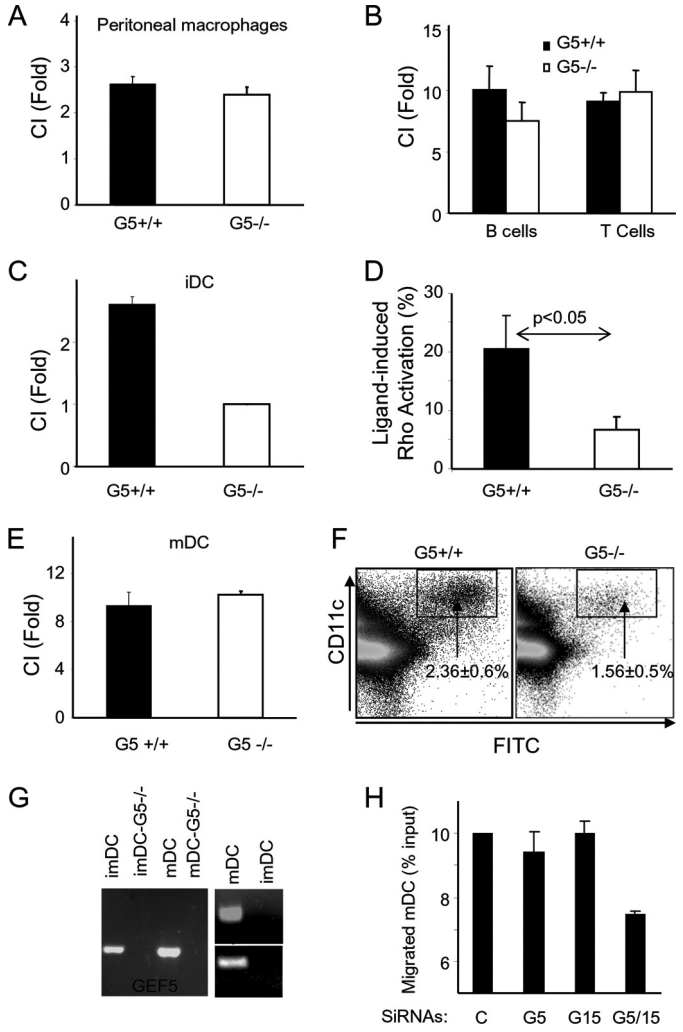

FIGURE 4. **Arhgef5 has an important role in immature DC migration.** *A–C*, transwell migration assays. Chemotactic activity of peritoneal macrophages (*A*), spleen T and B lymphocytes (*B*), and bone marrow-derived immature DCs (*C*) from wild type (*G5*+/+) or Arhgef5-deficient (*G5*−/−) mice was determined using the transwell assay. C5a (10 ng/ml, *A*), SDF-1 (100 ng/ml, *B*), and MIF1α (300 ng/ml, *C*) were used. *D*, RhoA activity in immature DCs. MIP-1α-induced Rho activation was determined using an ELISA kit that determines the levels of active RhoA. $p = 0.012$. *E*, transwell migration assay of bone marrow-derived mature DCs in response to CCL19 (60 ng/ml). *F*, *in vivo* migration of DCs. Mice were painted with FITC and cells from inguinal lymph nodes were isolated and stained with CD11c. The percentage of DCs migrated from the skins (FITC/CD11c double positive) were determined by flow cytometry. $n = 14$, $p < 0.05$. *G*, expression of Arhgef5 and its close homologs Arhgef15 and Ephexin-1 detected by RT-PCR in immature DCs (*imDC*) and mature DCs (*mDC*). *H*, knocking down of both Arhgef5 and -15 reduces migration of bone marrow-derived mature DCs in response to CCL-19. Bone marrow-derived mature DCs were transfected with no oligo (*C*) or synthetic siRNA oligos targeting Arhgef5 (*G5*), Arhgef15 (*G15*), or both (*G5/15*). $p < 0.05$, *fourth bar versus* others. *P* values for other bars are >0.05.

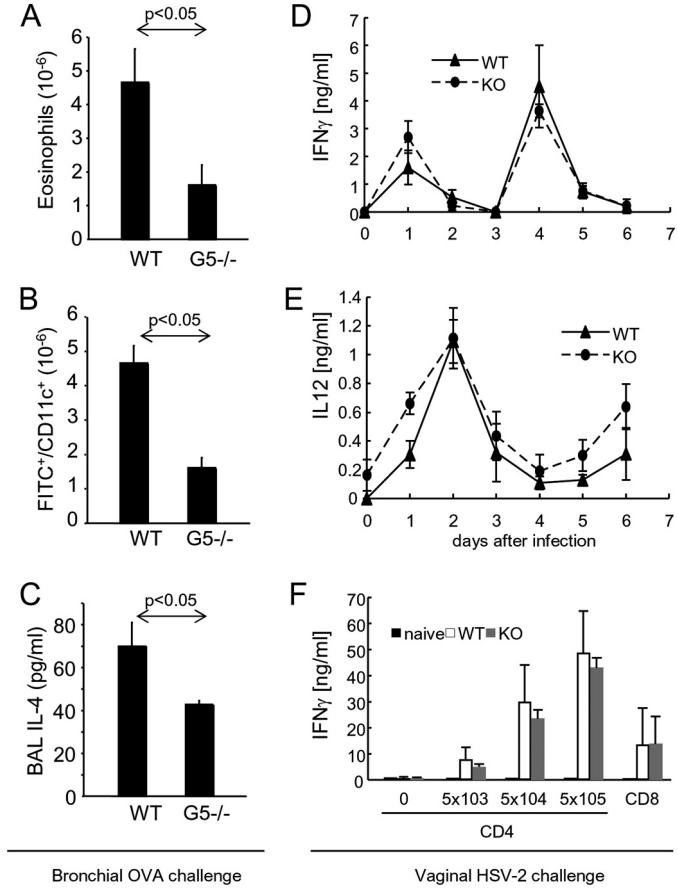

FIGURE 5. **Effects of Arhgef5 deficiency on two *in vivo* disease models.** *A–C*, effects of Arhgef5 deficiency on an OVA-induced allergic airway inflammation model. The numbers of eosinophils in BAL (*A*) and FITC$^+$/CD11C$^+$ cells in the bronchial lymph nodes (*B*) and the levels of IL-4 in BAL (*C*) were determined, $n = 7$. *D–F*, effects of Arhgef5 deficiency on a HSV-2 infection model. The levels of IFN-γ (*D*) and IL-12 (*E*) in vaginal washes were collected daily and determined. CD4$^+$ or CD8$^+$ T cells were isolated from iliac and inguinal lymph nodes. They were co-cultured with naïve wild type (*WT*) splenocytes and heat-inactivated HSV-2 of the indicated plaque-forming units (for CD4$^+$ T cells) or 1 μg/ml gB peptide (for CD8$^+$ T cells) for 3 days. The levels of IFN-γ in the conditioned medium were determined by ELISA (*F*). $n = 3$ (wild type) or 4 (*Arhgef5*−/−).

tured myeloid cells. By studying of Arhgef5-null mice, we demonstrated that Arhgef5 is a RhoA regulator *in vivo* and has an important role in the regulation of immature mouse DC chemotaxis. Together with the finding that Arhgef5 is directly activated by G$\beta\gamma$, we have characterized a novel signaling pathway from chemokine receptors to RhoA activation for regulation of leukocyte migration. In this signaling pathway, chemokine receptors presumably act through the G$\beta\gamma$ subunits of the G_i proteins to activate Arhgef5, which in turn activates RhoA. RhoA are known to regulate the formation and contractility of the actomyosin structure that provides a pushing force for leukocyte migration.

In this report, we provide strong evidence showing that Arhgef5 is directly regulated by G$\beta\gamma$. G$\beta\gamma$ binds to the linker region between the DH and PH domains of Arhgef5 as well as part of the PH domain. Arhgef5 is the first RhoA GEF that has been found to be directly regulated by G$\beta\gamma$. G$\beta\gamma$ may regulate Arhgef5 through a mechanism similar to that by which Gα_q regulates p63Rho-GEF revealed by a recent structural study (40). It is also possible that G$\beta\gamma$ may induce Arhgef5 membrane translocation as it does to a Rac-specific GEF, P-Rex1 (41). Additional studies, particularly structural ones, are needed to further determine the molecular mechanisms by which G$\beta\gamma$ regulates Arhgef5 activity.

The study of Arhgef5-null mice revealed that Arhgef5 is a significant regulator of RhoA in immature DCs. This observation is consistent with the effect of Arhgef5 deficiency on immature DC migration. Because of the up-regulation of Arhgef5 homologs in mature DCs, as shown in Fig. 4*G*, Arhgef5 is no

longer the primary GEF for RhoA regulation, and hence its deficiency no longer has a significant impact on mature DC migration. Immature DCs, once activated by antigens, start to migrate toward lymph nodes accompanied by their maturation process. It is reasonable to speculate that up-regulation of Arhgef5 homolog expression upon DC maturation would mask some of the *in vivo* effects of Arhgef5 deficiency. This molecular redundancy may help to explain the differential effects of Arhgef5 deficiency on the two model studies shown in Fig. 5. DCs are known to play important roles in both of the model systems, even though these two models are primarily mediated by T_h1 and T_h2 cells, respectively. The lack of significant effects of Arhgef5 deficiency on the responses in the HSV-2 infection model may be due to early maturation of DCs or an involvement of different types of DCs in which Arhgef5 has no primary role. In fact, DCs are rapidly activated through innate recognition of HSV-2 virions through TLR9 (42), and inflammatory monocytes are recruited to the site of infection and there differentiate into DCs (43). Although significant reduction in DC infiltration into the bronchial lymph nodes observed in Arhgef5-null mice should contribute to the reduction in eosinophil infiltration and IL-4 production in the OVA-induced asthma model, our results do not exclude other possible contributions by Arhgef5 deficiency to the attenuation of allergic airway inflammatory responses. Further studies are needed to clarify these questions. In addition, the presence of Ephexin-1 and Arhgef15 in neutrophils and macrophages (data not shown) may explain why Arhgef5 deficiency failed to affect migration of these leukocytes in response to chemoattractants. Inactivation of additional GEFs in this class may be needed to reveal if these GEFs are actually involved in chemotaxis of these leukocytes and to more comprehensively investigate the significance of this signaling pathway in immune responses *in vivo*.

REFERENCES

1. Ridley, A. J. (2001) *J. Cell Sci.* **114,** 2713–2722
2. Etienne-Manneville, S., and Hall, A. (2002) *Nature* **420,** 629–635
3. Allen, W. E., Zicha, D., Ridley, A. J., and Jones, G. E. (1998) *J. Cell Biol.* **141,** 1147–1157
4. Srinivasan, S., Wang, F., Glavas, S., Ott, A., Hofmann, F., Aktories, K., Kalman, D., and Bourne, H. R. (2003) *J. Cell Biol.* **160,** 375–385
5. Meili, R., and Firtel, R. A. (2003) *Cell* **114,** 153–156
6. Gu, Y., Filippi, M. D., Cancelas, J. A., Siefring, J. E., Williams, E. P., Jasti, A. C., Harris, C. E., Lee, A. W., Prabhakar, R., Atkinson, S. J., Kwiatkowski, D. J., and Williams, D. A. (2003) *Science* **302,** 445–449
7. Xu, J., Wang, F., Van Keymeulen, A., Herzmark, P., Straight, A., Kelly, K., Takuwa, Y., Sugimoto, N., Mitchison, T., and Bourne, H. R. (2003) *Cell* **114,** 201–214
8. Ridley, A. J. (2001) *Trends Cell Biol.* **11,** 471–477
9. Burridge, K., and Wennerberg, K. (2004) *Cell* **116,** 167–179
10. Wennerberg, K., and Der, C. J. (2004) *J. Cell Sci.* **117,** 1301–1312
11. Schwartz, M. (2004) *J. Cell Sci.* **117,** 5457–5458
12. Li, Z., Hannigan, M., Mo, Z., Liu, B., Lu, W., Wu, Y., Smrcka, A. V., Wu, G., Li, L., Liu, M., Huang, C. K., and Wu, D. (2003) *Cell* **114,** 215–227
13. Welch, H. C., Coadwell, W. J., Ellson, C. D., Ferguson, G. J., Andrews, S. R., Erdjument-Bromage, H., Tempst, P., Hawkins, P. T., and Stephens, L. R. (2002) *Cell* **108,** 809–821
14. Welch, H. C., Condliffe, A. M., Milne, L. J., Ferguson, G. J., Hill, K., Webb, L. M., Okkenhaug, K., Coadwell, W. J., Andrews, S. R., Thelen, M., Jones, G. E., Hawkins, P. T., and Stephens, L. R. (2005) *Curr. Biol.* **15,** 1867–1873
15. Dong, X., Mo, Z., Bokoch, G., Guo, C., Li, Z., and Wu, D. (2005) *Curr. Biol.* **15,** 1874–1879
16. Schmidt, A., and Hall, A. (2002) *Genes Dev.* **16,** 1587–1609
17. García-Mata, R., and Burridge, K. (2007) *Trends Cell Biol.* **17,** 36–43
18. Rossman, K. L., Der, C. J., and Sondek, J. (2005) *Nat. Rev. Mol. Cell Biol.* **6,** 167–180
19. Buchsbaum, R. J. (2007) *J. Cell Sci.* **120,** 1149–1152
20. Erickson, J. W., and Cerione, R. A. (2004) *Biochemistry* **43,** 837–842
21. Obermeier, A., Ahmed, S., Manser, E., Yen, S. C., Hall, C., and Lim, L. (1998) *EMBO J.* **17,** 4328–4339
22. Bagrodia, S., Bailey, D., Lenard, Z., Hart, M., Guan, J. L., Premont, R. T., Taylor, S. J., and Cerione, R. A. (1999) *J. Biol. Chem.* **274,** 22393–22400
23. Brummelkamp, T. R., Bernards, R., and Agami, R. (2002) *Science* **296,** 550–553
24. Ogita, H., Kunimoto, S., Kamioka, Y., Sawa, H., Masuda, M., and Mochizuki, N. (2003) *Circ. Res.* **93,** 23–31
25. Shamah, S. M., Lin, M. Z., Goldberg, J. L., Estrach, S., Sahin, M., Hu, L., Bazalakova, M., Neve, R. L., Corfas, G., Debant, A., and Greenberg, M. E. (2001) *Cell* **105,** 233–244
26. Xie, X., Chang, S. W., Tatsumoto, T., Chan, A. M., and Miki, T. (2005) *Cell Signal.* **17,** 461–471
27. Ellerbroek, S. M., Wennerberg, K., Arthur, W. T., Dunty, J. M., Bowman, D. R., DeMali, K. A., Der, C., and Burridge, K. (2004) *Mol. Biol. Cell* **15,** 3309–3319
28. Ren, X. D., Kiosses, W. B., and Schwartz, M. A. (1999) *EMBO J.* **18,** 578–585
29. Aspenström, P., Fransson, A., and Saras, J. (2004) *Biochem. J.* **377,** 327–337
30. Benard, V., Bohl, B. P., and Bokoch, G. M. (1999) *J. Biol. Chem.* **274,** 13198–13204
31. Gumienny, T. L., Brugnera, E., Tosello-Trampont, A. C., Kinchen, J. M., Haney, L. B., Nishiwaki, K., Walk, S. F., Nemergut, M. E., Macara, I. G., Francis, R., Schedl, T., Qin, Y., Van Aelst, L., Hengartner, M. O., and Ravichandran, K. S. (2001) *Cell* **107,** 27–41
32. Feng, Q., Baird, D., and Cerione, R. A. (2004) *EMBO J.* **23,** 3492–3504
33. Meller, N., Irani-Tehrani, M., Kiosses, W. B., Del Pozo, M. A., and Schwartz, M. A. (2002) *Nat. Cell Biol.* **4,** 639–647
34. Hill, C. S., Wynne, J., and Treisman, R. (1995) *Cell* **81,** 1159–1170
35. Mao, J., Yuan, H., Xie, W., Simon, M. I., and Wu, D. (1998) *J. Biol. Chem.* **273,** 27118–27123
36. Li, Z., Paik, J. H., Wang, Z., Hla, T., and Wu, D. (2005) *Prostaglandins Other Lipid Mediat.* **76,** 95–104
37. Remmers, A. E., Posner, R., and Neubig, R. R. (1994) *J. Biol. Chem.* **269,** 13771–13778
38. Mellman, I., and Steinman, R. M. (2001) *Cell* **106,** 255–258
39. Burns, S., and Thrasher, A. J. (2004) *Curr. Biol.* **14,** R965–R967
40. Lutz, S., Shankaranarayanan, A., Coco, C., Ridilla, M., Nance, M. R., Vettel, C., Baltus, D., Evelyn, C. R., Neubig, R. R., Wieland, T., and Tesmer, J. J. (2007) *Science* **318,** 1923–1927
41. Barber, M. A., Donald, S., Thelen, S., Anderson, K. E., Thelen, M., and Welch, H. C. (2007) *J. Biol. Chem.* **282,** 29967–29976
42. Lund, J., Sato, A., Akira, S., Medzhitov, R., and Iwasaki, A. (2003) *J. Exp. Med.* **198,** 513–520
43. Iijima, N., Linehan, M. M., Saeland, S., and Iwasaki, A. (2007) *Proc. Natl. Acad. Sci. U.S.A.* **104,** 19061–19066
44. Lutz, M. B., Kukutsch, N., Ogilvie, A. L., Rössner, S., Koch, F., Romani, N., and Schuler, G. (1999) *J. Immunol. Methods* **223,** 77–92
45. Rojas, R. J., Kimple, R. J., Rossman, K. L., Siderovski, D. P., and Sondek, J. (2003) *Comb. Chem. High Throughput Screen* **6,** 409–418
46. Macatonia, S. E., Knight, S. C., Edwards, A. J., Griffiths, S., and Fryer, P. (1987) *J. Exp. Med.* **166,** 1654–1667
47. Sato, A., and Iwasaki, A. (2004) *Proc. Natl. Acad. Sci. U.S.A.* **101,** 16274–16279